

# The Mechanical and Electrochemical Properties of DC-Electrodeposited Ni-Mn Alloy Coating with Low Internal Stress

Chun-Ying Lee, Kuan-Hui Cheng, Mei-Wen Wu

**Abstract**—The nickel-manganese (Ni-Mn) alloy coating prepared from DC electrodeposition process in sulphamate bath was studied. The effects of process parameters, such as current density and electrolyte composition, on the cathodic current efficiency, microstructure, internal stress and mechanical properties were investigated. Because of its crucial effect on the application to the electroforming of microelectronic components, the development of low internal stress coating with high leveling power was emphasized. It was found that both the coating's manganese content and the cathodic current efficiency increased with the raise in current density. In addition, the internal stress of the deposited coating showed compressive nature at low current densities while changed to tensile one at higher current densities. Moreover, the metallographic observation, X-ray diffraction measurement, and polarization curve measurement were conducted. It was found that the Ni-Mn coating consisted of nano-sized columnar grains and the maximum hardness of the coating was associated with (111) preferred orientation in the microstructure. The grain size was refined along with the increase in the manganese content of the coating, which accordingly, raised its hardness and resistance to annealing softening. In summary, the Ni-Mn coating prepared at lower current density of 1-2 A/dm<sup>2</sup> had low internal stress, high leveling power, and better corrosion resistance.

**Keywords**—DC plating, internal stress, leveling power, Ni-Mn coating.

## I. INTRODUCTION

THE electrodeposition process has been extensively applied in the fabrication of microelectronic devices [1]. Defect-free, high throughput, low dimensional distortion, high conformity and good mechanical property are some of the important requirements for this manufacturing method. For instance, the probes in probe card should have high strength for fatigue loading, high hardness for penetrating the oxide coating on the bump pad, low internal stress to minimize the dimensional distortion, fair corrosion resistance to reduce the environmental influences, and good aging property to withstand the heating due to testing current, etc. [2]. Nickel alloy coating has much improved strength and toughness than

monolithic nickel coating [3], [4]. Among the nickel alloys, Ni-Mn alloy has been reported as one of the potential candidates having good mechanical properties [5]. However, the mechanical properties of Ni-Mn alloy still depends on its compositions and microstructure [6]-[9], the tailoring of coating for specific application must still be performed.

The use of Ni-Mn alloy for electroforming is first proposed by Stephenson and coworkers [10], [11]. The effects of several plating parameters, such as manganese ion content, current density, temperature, and pH, were investigated. It was found that the hardness and internal stress increased with the Mn content in the coating. Recently, because the Ni-Mn alloy plating in nickel sulphamate bath had lower internal stress than Watt's bath, the former bath was adopted by most studies in the literature [12]-[18]. By comparing the processes of DC and pulse plating, Kelly and Goods concluded the former could prepare coating with higher strength [19]. Although the Mn content in the coating is usually less than 2 wt%, the hardness of coating can reach 500 Hv. However, when the Mn content was more than 1 wt.%, the coating became brittle and its structural application was limited [10]. The microstructure of the coating was nanocrystalline or amorphous at high Mn content [20], [21]. Annealing could recover the ductility with softening in hardness, but only at temperature higher than 300°C. At lower temperatures, a certain degree in age hardening was observed, which would be beneficial for probe card application because of the ohmic heating effect resulted from the applied current.

Although there are some detailed studies of the Ni-Mn alloy coating in the previously mentioned literature, the discussion on the control of low internal stress is still required for the microelectronic applications. In addition, the control of Mn content in the deposited alloy with the plating parameters is still not fully discussed, especially for the application in micro-probe structure with high leveling power. It is, thus, the goal of this study to investigate the plausible fabrication process for Ni-Mn structure with high strength, high leveling power and low internal stress by controlling the electrolyte bath and current density in the electrodeposition.

## II. EXPERIMENTAL

### A. Electrodeposition

As mentioned in the literature, Ni alloy plating in sulphamate bath is usually low in internal stress. Therefore, a nickel sulphamate bath with manganese chloride as the major source

Chun-Ying Lee is with the Department of Mechanical Engineering, National Taipei University of Technology, Taipei 10608, Taiwan (phone: 886-2-87731614; fax: 886-2-27317191; e-mail: leech@ntut.edu.tw).

Kuan-Hui Cheng is with the Graduate Institute of Manufacturing Technology, National Taipei University of Technology, Taipei 10608, Taiwan (phone: 886-2-27712171; fax: 886-2-27317191; e-mail: rr790620@Hotmail.com).

Mei-Wen Wu is with the General Education Department, Chienkuo Technology University, Changhua 50015, Taiwan (e-mail: mwwu@cc.ctu.edu.tw).

of Mn ions was adopted in this study [22], [23]. Table I presents the bath compositions and associated plating parameters used in this study. The copper substrate was in dimensions of 8 cm × 3.25 cm. Before the electroplating, the substrate was pretreated with degreaser, de-ionized water, and diluted sulfuric acid to clean and activate the cathode surface. On the other hand, S-round nickel disks bagged in non-woven cloth and titanium basket were used as the anode. The coating was deposited with a nominal thickness of 50 μm. After electrodeposition, the specimen was weighted and the current efficiency was calculated by using Faraday's theorem.

TABLE I  
BATH COMPOSITIONS AND PLATING PARAMETERS

Parameter	Magnitude
nickel sulphamate	Ni <sup>2+</sup> : 90 g/l
manganese sulfate, MnSO <sub>4</sub> •5H <sub>2</sub> O	Mn <sup>2+</sup> : 10 g/l
nickel chloride, NiCl <sub>2</sub> •6H <sub>2</sub> O	3 g/l
boric acid, H <sub>3</sub> BO <sub>3</sub>	40 g/l
sodium dodecyl sulfonate (SDS), C <sub>12</sub> H <sub>25</sub> SO <sub>3</sub> Na	1.8 ml/l
pH	3.5-4.0
temperature	50°C
magnetic stirring speed	200 rpm
current density	0.2-12 A/dm <sup>2</sup>

### B. Microstructure Examination

One of the functions of surface coating is to improve the finish of workpiece. This ability of the plating process is measured by the leveling power. A substrate surface with grooved pattern, cross-section as shown schematically in Fig. 1, was electrodeposited. At equal plating intervals, a thin layer of copper was plated in order to record the evolution of the specimen surface. The leveling power (LP) was defined as [24]:

$$LP(\%) = \frac{h_r - h_p}{d_0} \times 100\% \quad (1)$$

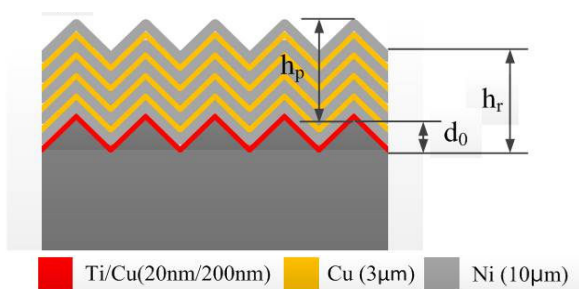


Fig. 1 Schematic diagram on the cross-section of specimen for leveling power measurement

In (1),  $d_0$  is the depth of the peak and root of the original groove pattern, and  $h_p$  and  $h_r$  are the deposition thicknesses at the peak and root, respectively. More specifically,  $L_p=0$  and  $L_p=100\%$  correspond to no leveling of the groove pattern at all and complete final flat surface, respectively. In this study, grooves of  $d_0=50\mu\text{m}$  and  $90^\circ$  ridge angle were prepared on Si wafer.

The crystalline structure of the coating was examined by employing x-ray diffractometer (MAC Science M03XHF,

$\lambda=0.15416$  nm). The corresponding grain size was calculated by the Scherrer formula based on full width at half maximum of the diffraction peak. For the composition analysis, an electron probe x-ray microanalyzer (EPMA, JEOL JXA-8200) was used. Moreover, scanning electron microscope (SEM, JEOL JSM-7401F) was used for the surface morphology examination of the coating.

### C. Property Measurement

A flexural stripe cathode specimen (PN 1194, Specialty Testing & Development Co.) was employed in the internal stress measurement. In order to minimize the coating effect, the thickness of coating was controlled within 3 μm. For the hardness measurement, the polished specimen was tested with a Vickers hardness tester under 50 g of loading and 15 s of loading duration. As for the measurement of coating's corrosion resistance, the polarization curve was obtained from a potentiostat (Jie-han 5000 Electrochemical Workstation).

## III. RESULTS AND DISCUSSION

### A. Surface morphology

Fig. 2 shows the surface SEM morphologies of the coatings deposited at three different current densities: 4, 8, and 12 A/dm<sup>2</sup>, respectively. Basically, the surfaces were smooth with small grains. However, both coatings deposited at 8 and 12 A/dm<sup>2</sup> developed cracking. For higher current density, the cracking was more serious and easier to be observed.

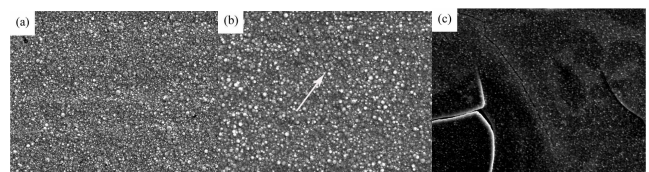


Fig. 2 SEM surface morphology of the coating deposited at different current density: (a) 4 A/dm<sup>2</sup>, (b) 8 A/dm<sup>2</sup>, (c) 12 A/dm<sup>2</sup>

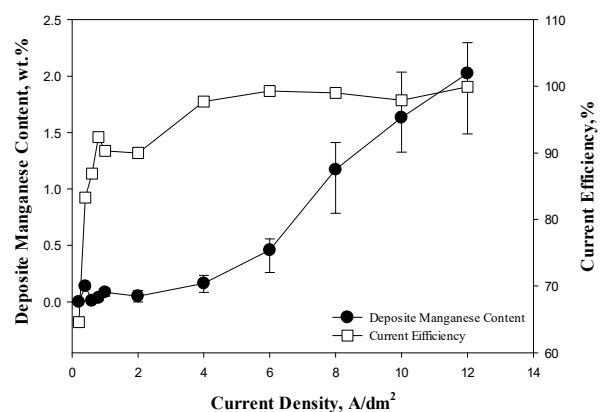


Fig. 3 The changes of current efficiency and coating's Mn content with respect to the current density applied in deposition

### B. Current Efficiency

Current efficiency denotes the efficiency with which charge are transferred in a system facilitating an electrochemical reaction, the higher efficiency and the faster production rate.

The changes in current efficiency along with the Mn content in the coating with respect to deposition current density are shown in Fig. 3. It is noted that current efficiency increased with current density. For the current density higher than 4 A/dm<sup>2</sup>, the deposition had nearly reached 100% efficiency. The lower current efficiency at low current density should be related to the low overpotential used in the deposition. Moreover, the higher overpotential at high current density should also facilitate the codeposition of Mn. Therefore, the Mn content in the coating increased with the current density. At 12 A/dm<sup>2</sup>, the Mn content reached 2 wt.%, which was relatively high compared with the results reported in the literature.

### C. Internal Stress

For the coatings prepared at different current densities, the internal stress changed drastically, as shown in Fig. 4. The results in Fig. 4 denoted that the internal stress evolved from compressive to tensile as the current density increased. The slightly decreased internal stress at current density higher than 8 A/dm<sup>2</sup> was due to the stress relaxation of coating cracking, as seen in Fig. 2. The increase in internal stress with the current density was consistent with the finding in literature [25]. Also shown in Fig. 4 is the variation of coating hardness with respect to current density. The hardness increased nearly linearly with the current density, with a special jump at 1 A/dm<sup>2</sup>. This singularity will be discussed later on. For coating prepared by electrodeposition, high current density means high overpotential in the reduction reaction. High overpotential thus results in refined grain and higher hardness.

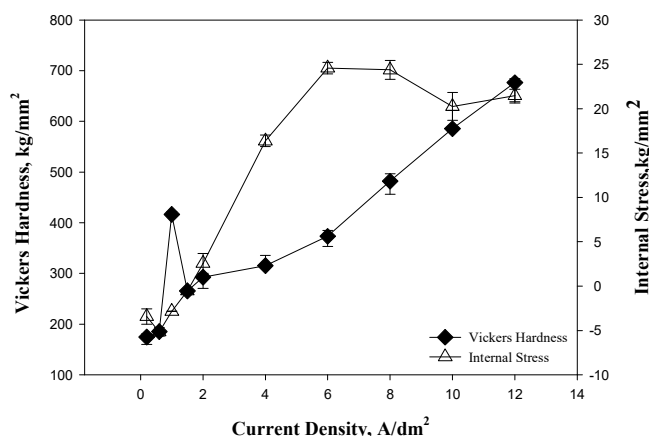


Fig. 4 The measured internal stress and hardness of the coating prepared at different current densities

### D. XRD Spectra

Fig. 5 presents the XRD spectra of the coatings prepared at different current densities. It can be seen that all coatings were FCC crystalline with preferred orientation at (200) except those coatings prepared at 1 A/dm<sup>2</sup> and 12 A/dm<sup>2</sup>. The relatively higher hardness for the coating deposited at 1 A/dm<sup>2</sup>, as seen in Fig. 4, should be resulted from this (111) texture which is closest packed crystallographic plane having maximum in-plane elastic modulus [26]. In order to further understand the microstructures of the coatings, optical micrographs were taken

on their cross-sections and shown in Fig. 6. When the current density was low, equiaxed granular structure was seen. These equiaxed grains changed into columnar as the current density increased. However, at current density around 1 A/dm<sup>2</sup>, the columnar characteristic was weakened. The columnar grains reappeared as current density further increased. Finally, at 12 A/dm<sup>2</sup>, layer-like structure was observed.

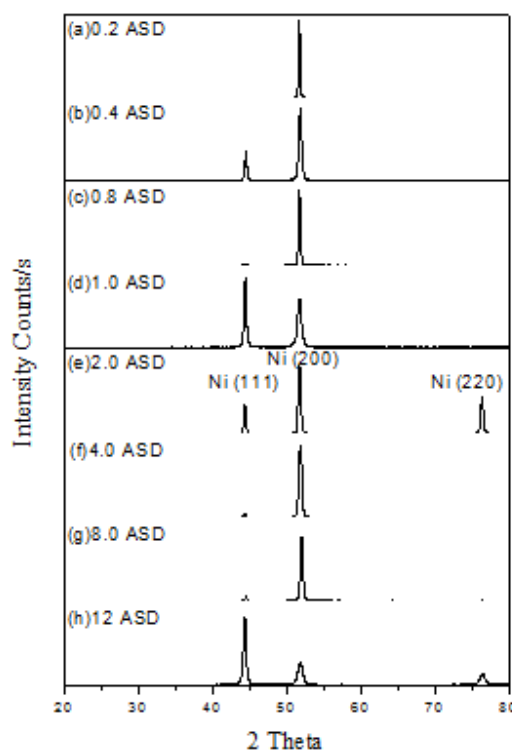


Fig. 5 XRD spectra of the coatings prepared at different current densities: (a)0.2 A/dm<sup>2</sup>, (b)0.4 A/dm<sup>2</sup>, (c)0.8 A/dm<sup>2</sup>, (d)1.0 A/dm<sup>2</sup>, (e)2.0 A/dm<sup>2</sup>, (f)4.0 A/dm<sup>2</sup>, (g)8.0 A/dm<sup>2</sup>, (h)12 A/dm<sup>2</sup>

### E. Annealing Effect

When the Ni-Mn alloy was used in the microelectronic applications, the carried current through its structure could cause temperature rise due to ohmic heating. Therefore, the material behavior at elevated temperature was concerned. Fig. 7 presents the change in hardness of the coating after 1-hr annealing treatment at 200°C. It appeared that both softening and hardening occurred depending on the current density used in the deposition. When the current density was lower than 2 A/dm<sup>2</sup>, softening occurred in the coating after annealing. But as current density was higher than 2 A/dm<sup>2</sup>, precipitation hardening was observed. It is believed that the higher Mn content in the coating can delayed recrystallization more effectively and precipitation of the dissolved Mn can generate the aging effect.

### F. Leveling Power

To improve the surface finish of coating, the leveling power of the plating system is crucial. Fig. 8 shows the cross-sections of grooved specimens after deposition. For comparison between the Ni and Ni-Mn coatings, Fig. 8 (a) presents the

result of Ni coating whereas Figs. 8 (b)-(d) represent the results of Ni-Mn coatings prepared at different current densities. The corresponding leveling power of Ni-Mn coating was calculated based on (1) and plotted in Fig. 9. The leveling power of Ni coating calculated from Fig. 8 (a) was around 10%, which was much lower those of Ni-Mn coatings at low current density. The suppression of electric flux around the electric field concentration site by manganese ions should be the underlined mechanism for this improvement [27]. However, this improvement diminished with increasing current density. Although the leveling power at 8 A/dm<sup>2</sup> increased back to 80%, the entrapped cavities in the coating, as seen in Fig. 8 (d), would be serious defects for application. Therefore, the deposition of Ni-Mn coating at 2 A/dm<sup>2</sup> had better leveling power to heal the surface irregularities of specimen.

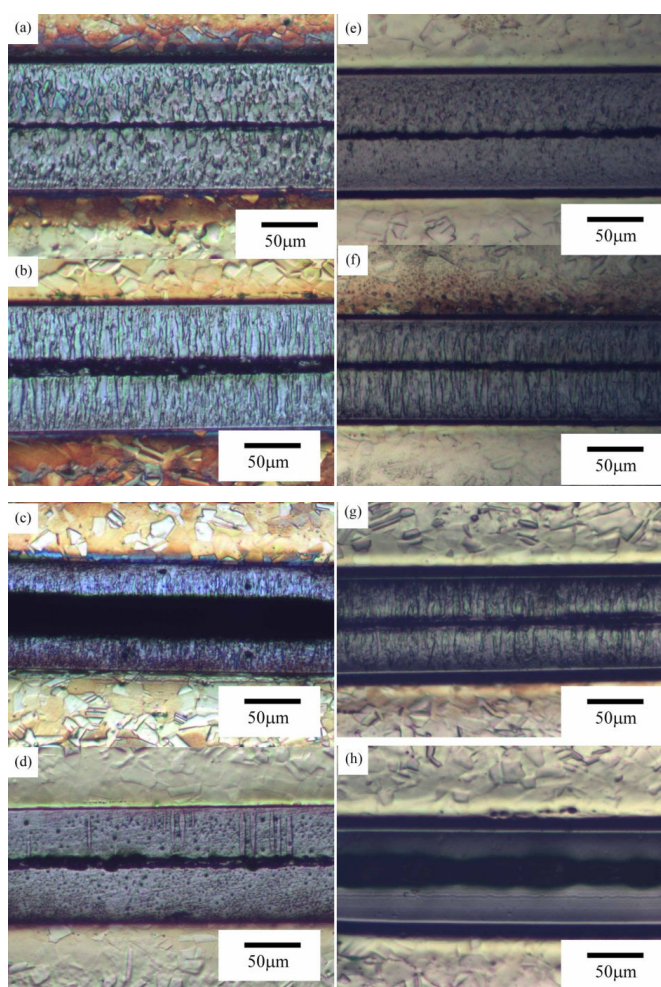


Fig. 6 Optical micrographs on the cross-section of the coatings deposited at different current densities: (a)0.2 A/dm<sup>2</sup>, (b)0.6 A/dm<sup>2</sup>, (c)0.8 A/dm<sup>2</sup>, (d)1.0 A/dm<sup>2</sup>, (e)2 A/dm<sup>2</sup>, (f)6 A/dm<sup>2</sup>, (g)8 A/dm<sup>2</sup>, (h)12 A/dm<sup>2</sup>

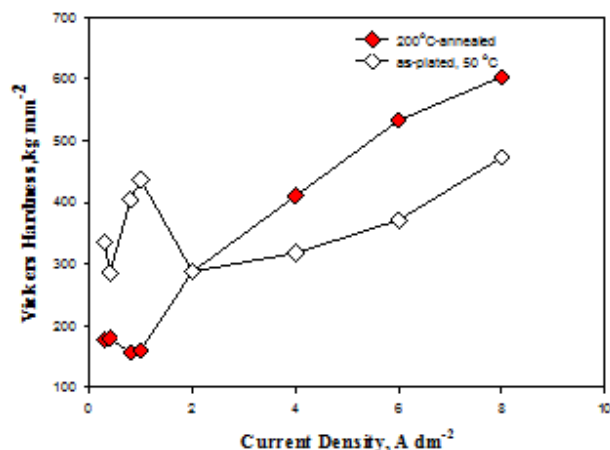


Fig. 7 The comparison in the measured hardness for coatings with and without 200°C annealing

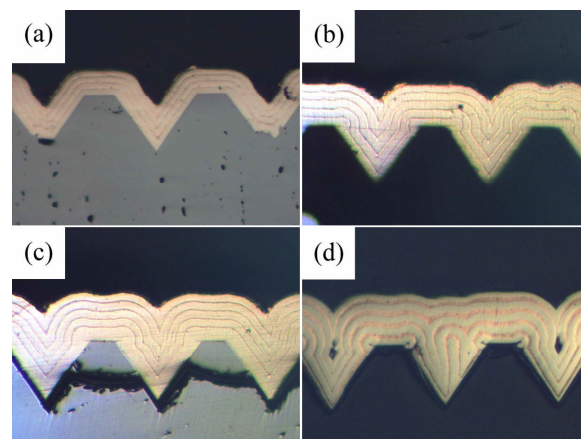


Fig. 8 Cross-sections of grooved specimens after deposition: (a)Ni coating, (b) Ni-Mn coating at 0.4 A/dm<sup>2</sup>, (c) Ni-Mn coating at 2.0 A/dm<sup>2</sup>, (d) Ni-Mn coating at 8.0 A/dm<sup>2</sup>

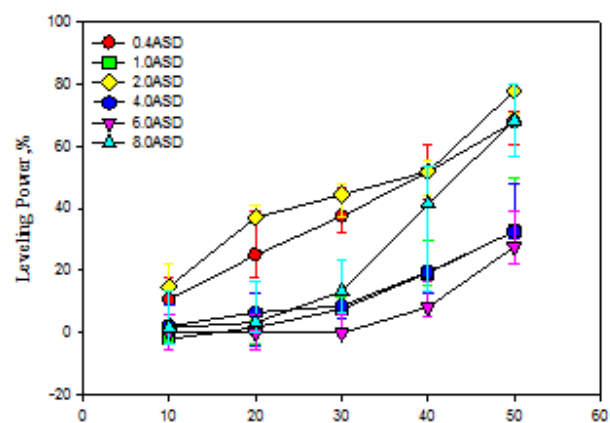


Fig. 9 The changes of leveling power with coating thickness for Ni-Mn coatings prepared at different current densities

### G. Electrochemical Property

The potentiodynamic polarization curve of the coating was measured in 0.5 M sulfuric acid solution. Based on the Tafel extrapolation on the polarization curve, the corrosion current  $I_{corr}$  and corrosion potential  $E_{corr}$  were obtained. Table II

presents  $I_{\text{corr}}$  and  $E_{\text{corr}}$  of the coatings prepared at different current densities. It is seen that the coating prepared at  $1 \text{ A/dm}^2$  had the lowest  $I_{\text{corr}}$  and highest  $E_{\text{corr}}$ . In other words, Ni-Mn coating deposited at low current density had better corrosion resistance. The corrosion currents were lower than that of Ni coating. By referring to Fig. 3, it is realized that even minor Mn content in the coating can improve its corrosion resistance. At high current density, the Ni-Mn coating deteriorated its corrosion resistance significantly. This should relate to the intensive surface cracking of the Ni-Mn coating developed due to high internal stress, as seen in Fig. 2. The low internal stress for the coating prepared at  $1 \text{ A/dm}^2$  should also contribute to its excellent performance in corrosion resistance.

TABLE II  
CORROSION CURRENT AND POTENTIAL OF COATINGS PREPARED AT DIFFERENT CURRENT DENSITIES

Coating	Current Density ( $\text{A/dm}^2$ )	$I_{\text{corr}}(\mu\text{A/cm}^2)$	$E_{\text{corr}}(\text{V vs. SCE})$
Ni	1.0	7.1592	-0.30714
	0.2	0.5175	-0.37048
	1.0	0.0156	-0.23790
Ni-Mn	2.0	7.4839	-0.30499
	8.0	17.851	-0.30229
	10.0	60.567	-0.33084

#### IV. CONCLUSION

For its potential application in microelectronic industry, Ni-Mn alloy coating prepared in sulphamate bath with different DC current densities was investigated. It was found that only minor amount of Mn ( $< 2.0 \text{ wt.}\%$ ) was able to co-deposit into the Ni matrix. Nevertheless, the hardness could be effectively increased from 200 Hv to 700 Hv. When the current density was larger than  $2.0 \text{ A/dm}^2$ , the coating could even withstand the softening of  $200^\circ\text{C}$ -annealing. In addition, with the current density lower than  $2.0 \text{ A/dm}^2$ , the internal stress could be well controlled under  $5 \text{ kg/mm}^2$ , even compressive one appeared. In the aspect of leveling power of the deposition system, the Ni-Mn system prevailed over its monolithic Ni counterpart. However, leveling power decreased with the applied current density. As the corrosion resistance of the coating was concerned, the cracking due to high internal stress was detrimental to its performance. Ni-Mn coating prepared at low current density was therefore recommended. In general consideration, the Ni-Mn coating prepared at current density around  $1\text{-}2 \text{ A/dm}^2$  had low internal stress, fair hardness, high leveling power, and better corrosion resistance. It can be a plausible electrodeposition system in microelectronic applications.

#### ACKNOWLEDGMENT

The financial support from Ministry of Science and Technology, Taiwan, under Grant No. MOST 103 - 2221 - E - 027 - 019 is gratefully acknowledged.

#### REFERENCES

[1] L. T. Romankiw, "A Path: From Electroplating Through Lithographic Masks in Electronics to LIGA in MENS," *Electrochimica Acta*, vol. 41, no. 20-22, 1997, pp. 2985-3005.

[2] K. H. Cheng, F. J. Chen, C. Y. Lee, C. S. Lin, J. T. Huang, C. C. Lan, P. H. Tsou, T. I. Ho, "Fabrication of Ni-Mn Microprobe Structure with Low Internal Stress and High Hardness by Employing DC Electrodeposition," *Advances in Materials Science and Engineering*, vol. 2014, 2014, Article ID 890814, 6 pages.

[3] G. A. Malone, "New Developments in Electroformed Nickel-Based Structural Alloys," *Plating and Surface Finishing*, 1987, vol. 74, pp. 50-56.

[4] R. J. Tzou, H. S. Chou, "The Electroforming of Nickel-Based Alloys," *Journal of Chinese Corrosion Engineering*, vol.6, no.3,1992, pp.32-38

[5] N. Y. C. Yang, T. J. Headley, "Metallurgy of High Strength Ni-Mn Microsystems Fabricated by Electrodeposition," *Scripta Materialia*, vol.51, 2004, pp.761-766.

[6] A. V. Ryazhkin, Yu. A. Babanov, T. Miyahara, T. Ogasawara, K. Nitta, S. Ohwada, V. P. Pilyugin, A. M. Patchelov, E. G. Chernyishov, "Lattice Parameters for Ni-Mn Disordered Alloys by EXAFS," *Materials Science*, vol.12C, vol.22, 2005, pp.131.

[7] S. H. Goods, J. J. Kelly, N. Y. C. Yang, "Electrodeposited Nickel-Manganese: An Alloy for Microsystem Applications," *Microsystem Technologies*, vol.10, 2004, pp. 498-505.

[8] E. A. Marquis, A. A. Talin, "Effect of Current Density on the Structure of Ni and Ni-Mn Electrodeposits," *Journal of Materials Engineering*, vol.36, 2006, pp.669-676.

[9] N. Atanassov, V. Mitreva, "Electrodeposition and Properties of Nickel-Manganese Layers," *Surface & Coating Technology*, vol.78, 1996, pp. 144-149.

[10] W. B. Stephenson, Fermer Jr., "Development and Utilization of a High Strength Alloy for Electroform," *Plating*, vol. 52, no. 2, 1966, pp.183-192.

[11] W. B. Stephenson, Cincinnati, Jr., R. F. Edward, "Electrodeposition of a Nickel-Manganese Alloy," US Patent No. 3244603, 1968.

[12] A. Stephen, "Corrosion Behaviour of Electrodeposited Ni-Mn Alloys-Electrochemical Impedance Measurements," *Anti-Corrosion Methods and Materials*, Vol.46, no.2, 1999, pp.117-121.

[13] W. R. Wearmouth, K. C. Belt, "Electroforming with Heat-resistant, Sulfur-hardened Nickel," *Plating*, vol. 66, no. 10, 1979, pp.53-57.

[14] W. R. Wearmouth, "Hard, Heat-resistant Nickel Electrodeposits," US Patent No. 4108740, 1977.

[15] G. A. Malone, "Study of High Performance Alloy Electroforming," NASA-CR- 173828, US NTIS, 1984.

[16] G. A. Malone, "Study of High Performance Alloy Electroforming," NASA-CR- 175494, US NTIS, 1985.

[17] J. W. Dini, H. R. Johnson, "High-Temperature Ductility of Electrodeposited Nickel," SAND77-8020, US Sandia Laboratories.

[18] J. W. Dini, H. R. Johnson, L. A. West, "On the High-Temperature Ductility Properties of Electrodeposited Sulfamate Nickel," *Plating*, vol. 65, no. 2, 1978, pp.36-40.

[19] J. J. Kelly, S. H. Goods, "High Performance Nanostructured Ni-Mn Alloy for Microsystem Applications," *Electrochemical and Solid - State Letters*, vol.6, no.6, 2003, pp.C81 - C91.

[20] G. Lucadamo, D. L. Medlin, "Characterization of Twinning in Electrodeposited Ni-Mn Alloys," *Philosophical Magazine*, vol.85, vol.22, 2005, pp.2549 - 2560.

[21] F. J. Chen, "Study on Hexavalent Chromium Process Alternatives", Ph.D. Dissertation, Department of Mechanical Engineering, National Taiwan University, Taipei, Taiwan, Nov. 2009.

[22] Y. Tsuru, M. Nomura, "Effects of Chloride, Bromide and Iodide Ions on Internal Stress in Films Deposited during High Speed Nickel Electroplating from a Nickel Sulfamate Bath," *Journal of Applied Electrochemistry*, vol.30, 2000, pp.231 - 238.

[23] A. Stephen, "Magnetic Properties of Electrodeposited Nickel-Manganese Alloys: Effect of Ni/Mn Bath Ratio," *Journal of Applied Electrochemistry*, vol. 30, 2000, pp.1313 - 1316.

[24] M. Pushpavanam, V. Raman, "Leveling in Bright Nickel-Iron," *Metal Finishing*, vol. 84, no. 5, 1986, pp.51-55.

[25] S. J. Hearne, J. A. Floro, M. A. Rodriguez, R. T. Tissot, C. S. Frazer, L. Brewer, P. Hlava, and S. Foiles, "Stress Creation during Ni-Mn Alloy Electrodeposition," *Journal of Applied Physics*, vol.99, 2006, pp.053517\_1 - 053517\_4.

[26] M. A. Meyers and K. K. Chawla, *Mechanical Behavior of Materials*, Prentice Hall, New Jersey, US, 1999.

[27] C. W. Chu, "Effects of Manganese Doped Ba<sub>1.002</sub>(Ti<sub>0.82</sub>Zr<sub>0.18</sub>)O<sub>3</sub>+ $\delta$  on Insulation Resistance and Dielectric Properties," Master Thesis, Department of Materials Science and Engineering, National Cheng-Kung University, Tainan, Taiwan, June 2005.